Celest Mech Dyn Astr (2010) 106:1–24
DOI 10.1007/s10569-009-9235-0

ORIGINAL ARTICLE

Gravity assist space pruning based on differential algebra

R. Armellin · P. Di Lizia · F. Topputo · M. Lavagna · F. Bernelli-Zazzera · M. Berz

Received: 15 October 2008 / Revised: 30 September 2009 / Accepted: 1 October 2009 /
Published online: 24 November 2009

Abstract In this paper a differential algebra version of the gravity assist space pruning algorithm is presented. The use of differential algebraic techniques is proposed to overcome the two main drawbacks of the existing algorithm, i.e., the steep increase of the number of function evaluations with the number of planets involved in the transfer, and the use of a bounding procedure that relies on Lipschitzian tolerances. Differential algebra allows us to process boxes in place of grid points, and to substitute pointwise evaluations of the constraint functions with their Taylor expansions. Thanks to the particular instance of multi-gravity assist problems dealt with, all the planet-to-planet legs can be treated independently, and forward and backward constraining can be applied. The proposed method is applied to pre-process the search space of sample interplanetary transfers and it also serves as a stepping stone towards a fully rigorous treatment of the pruning process based on Taylor models.

Keywords Global optimization · Multi-gravity assist transfer · Search space pruning · Differential algebra techniques

R. Armellin · P. Di Lizia · F. Topputo (✉) · M. Lavagna · F. Bernelli-Zazzera
Dipartimento di Ingegneria Aerospaziale, Politecnico di Milano, Via La Masa 34, 20156 Milano, Italy
e-mail: topputo@aero.polimi.it

R. Armellin
e-mail: armellin@aero.polimi.it

P. Di Lizia
e-mail: dilizia@aero.polimi.it

M. Lavagna
e-mail: lavagna@aero.polimi.it

F. Bernelli-Zazzera
e-mail: bernelli@aero.polimi.it

M. Berz
Department of Physics and Astronomy, Michigan State University, East Lansing, MI 48824, USA
e-mail: berz@msu.edu

1 Introduction

Multi-gravity assist (MGA) transfers are usually made up by a sequence of planet-to-planet transfers in which the spacecraft exploits each planet encounter to achieve a velocity change by a gravity assist maneuver. A class of these trajectories can be preliminary designed in the frame of patched-conics approximation. In this context, different conic arcs are linked together to define the whole transfer trajectory. This paper focuses on a particular instance of patched-conics trajectories. More specifically, each planet-to-planet leg in the whole transfer is modeled as a conic arc, which is obtained as solution of a Lambert's problem (Battin 1987). Subsequent arcs are then linked together at the intermediate planet by means of a powered gravity assist maneuver (Labunsky et al. 1998). For the sake of brevity, this instance of interplanetary transfers is referred to as multi-gravity assist transfer in the remainder. Constructing MGA space trajectories is a well-known procedure in astrodynamics that has been used to reach both inner and outer planets.

The first MGA trajectories were designed using "ad hoc" methods developed for a specific mission. Approaching MGA problems from a global optimization standpoint has been proposed more recently. If the minimization of the propellant mass is concerned, MGA problems show an objective function with a large number of clustered minima (Di Lizia and Radice 2004; Vasile and De Pascale 2006), which are prevalently associated to the relative motion of the planets involved in the transfer. This causes classical local optimization methods to converge to one of these local minima (Betts 2001). Hence, despite their efficiency, local methods have to be avoided when looking for the global minimum of an MGA problem, at least in the first stage of the search process. Consequently, effective global optimization algorithms should be developed and used to find the best solution of an MGA problem.

Extensive work has been devoted to address the global optimization of MGA transfers, which was mainly based on global optimizers used as "black-box" tools. More specifically, an extensive test campaign was run, where stochastic (Yao 1997; Ingberg 1993; Sentinella and Casalino 2009), branch and bound (Jones et al. 1993), meta-model based (Jones 2001), and even combined (Vasile et al. 2005) methods were applied to the design of interplanetary transfers. Although some of them showed good performances in identifying the known best solutions for the test problems, a key point for the development of effective and more efficient algorithms was identified as the definition of global optimization strategies that are built to exploit the structure of the search space and the nature of the MGA problem (Di Lizia and Radice 2004).

It has recently been shown that the search space of MGA problems can be effectively pruned. This observation was successfully coded in the gravity assist space pruning (GASP) algorithm (Myatt et al. 2004). With GASP, the search space is pruned by exploiting imposed constraints. These are physical and technological constraints typical of an interplanetary trajectory (i.e., the minimum pericenter radius of fly-by hyperbolae and the maximum magnitude of impulse burns). Thanks to the particular class of interplanetary transfers dealt with, all planet-to-planet legs making up the whole transfer can be treated independently, and forward and backward constraining can be applied. In this way, the search space is pre-processed and global optimization algorithms are employed in the reduced domain. This procedure showed better performances if compared with the standard implementation of some stochastic global optimization solvers over the entire search space.

The classical implementation of GASP is based on a systematic evaluation of the objective and constraint functions on a grid of points distributed over the search space. This intrinsically involves a steep increase of the number of function evaluations with the number of planets involved in the transfer. Indeed, the grid must be kept sufficiently fine to avoid loosing

accuracy on the description of the shape of the constraint functions over the search space. Moreover, the pruning process relies on a bounding procedure that makes use of Lipschitzian tolerances, which must be either estimated or guessed in some way. It is worth noting that inaccurate estimations of this tolerance may lead to prune away feasible portions of the search space, and therefore to get rid of potential zones where the global minimum could lie. Thus, proper heuristics must be used to obtain good estimates, in order for the Lipschitzian tolerance to have only minor influence on the results.

In this paper we propose the use of differential algebraic (DA) techniques as a viable option to improve the GASP algorithm. DA techniques serve the purpose of automatic differentiation, i.e., the accurate computation of the derivatives of functions in a computer environment (Berz 1999b). More specifically, the classical implementation of the real algebra is substituted with the proper implementation of a new algebra based on Taylor polynomials. Given a generic function f of v variables, the Taylor expansion of f up to any desired order n with respect to all v variables can be easily obtained from a computer algorithm.

In the DA version of GASP the search space is split into boxes, processed in place of grid points, and the pointwise evaluation of the constraint functions is substituted by the computation of their Taylor expansion over the sampling boxes. In addition, a suitable devised polynomial bounder is used to estimate the ranges of the functions within each box. In this way guessing the Lipschitzian tolerance typical of the GASP method is avoided. Furthermore, the order of the Taylor expansion can be used to tune the accuracy of the approximation and the size of the grid boxes. This might result in the possibility of enlarging the grid for the domain discretization with a consequent reduction of the computational burden.

We point out that this paper is not aimed at formulating a novel global optimization strategy, but rather it addresses the pruning of the search space for a particular class of MGA transfers. In this context, a modification of classic GASP is presented, and the features of its DA version are discussed. The goals of the paper are:

1. to state the classic GASP algorithm into the perspective of DA formalism;
2. to derive a DA version of GASP requiring a fewer number of function evaluations and less computational effort than classic GASP;
3. to avoid the use of a Lipschitzian constant in the approximation of the constraint functions over the search space.

The paper is organized as follows. A short description of the method underlying GASP is given in Sect. 2. A brief introduction to differential algebra is given in Sect. 3. More specifically, being at the base of the algorithms presented in this work, the solution of parametric implicit equations using DA techniques is illustrated in Sect. 3.1. The algorithm for the Taylor expansion of the constraint functions typical of MGA transfers is described in Sect. 4. The main problems encountered introducing DA techniques into GASP are illustrated in Sect. 5, together with the adopted solutions. Finally, the assessment of the performances of the resulting algorithm is addresses in Sect. 6, based on MGA transfers of increasing complexity.

2 Gravity assist space pruning

GASP was originally introduced by Myatt et al. (2004) as a pruning strategy to design MGA transfers. As stated in Sect. 1, an MGA transfer is modeled as a sequence of conic arcs, each one patched to the subsequent one by a powered gravity assist maneuver. Consequently,

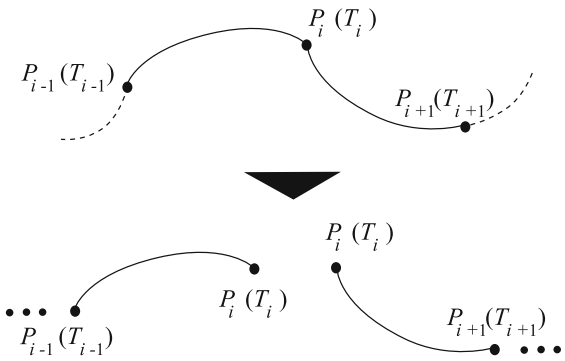

Fig. 1 Reduction of the MGA transfer to a cascade of two-dimensional subproblems

an MGA transfer involving n planets is an n-dimensional problem, as n variables are needed to identify the position of the planets at each gravity assist and, consequently, the conic arcs that define the trajectory. Referring to Fig. 1, the main idea behind GASP is splitting the whole trajectory in its elementary arcs. More importantly, if the epochs T_i of all the planet encounters are selected as design variables, each arc can be dealt with separately as a 2D problem defined by the two epochs necessary to compute the position of the departing and arrival planets.

For each two-dimensional subproblem, a set of constraints is usually available. These constraints can be gathered into three main groups:

- maximum allowed ΔV at departure (first arc) and arrival (last arc);
- maximum allowed corrective ΔV at each gravity assist;
- minimum allowed pericenter radius at each gravity assist.

The previous constraints can be profitably used to prune the search space. Consider, as an example, the first two arcs of an MGA transfer, which are fully characterized in the (T_1, T_2)- and (T_2, T_3)-plane, respectively (see Fig. 2). A uniform grid of points is built on each plane to sample the associated search space. For each point in the (T_1, T_2)-plane, the related constraint functions are evaluated. If any constraint is violated, the point is pruned away, together with all its subsequent combinations. In particular, if an entire row corresponding to an epoch $T_2 = \bar{T}_2$ is pruned away based on this analysis, then the entire column corresponding to $T_2 = \bar{T}_2$ in the (T_2, T_3)-plane can be pruned away as well, since $\bar{T}_2$ turns out to be an unfeasible value for T_2. Similar statements hold for the subsequent arcs. Consequently, thanks to the previous mechanism, constraints can be propagated forward and backward in the MGA transfer. The final result is a reduced search space, made up by feasible regions, where optimization tools are run. The reduced dimension of the search space improves the performances of the algorithms in this optimization phase.

As already pointed out in Sect. 1, the pruning process is performed on a grid of points distributed over the search space. Consequently, the grid must be kept sufficiently fine to accurately describe the constraint functions. Moreover, an estimate of the Lipschitzian constant is used to loosen the constraints, in order to compensate for the effects of the grid sampling of the search space. In particular, as a grid point is representative of its neighborhood on the search space, the Lipschitzian tolerance value must be estimated in accordance with grid spacing and functions properties to avoid the pruning of feasible regions.

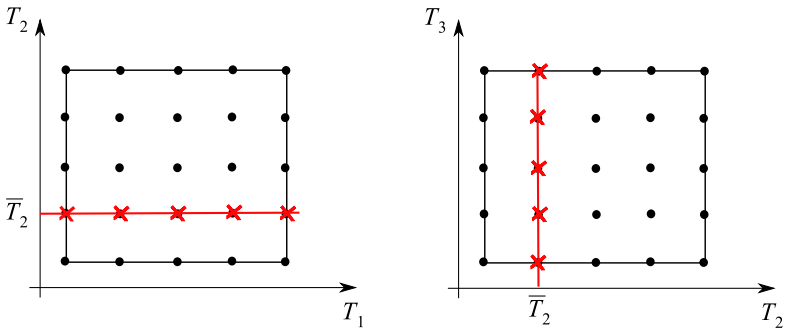

Fig. 2 Constraint propagation mechanism in GASP

3 Differential algebra

DA techniques find their origin in the attempt to solve analytical problems by an algebraic approach (Berz 1999b). Historically, the treatment of functions in numerics has been based on the treatment of numbers, and the classical numerical algorithms are based on the mere evaluation of functions at specific points. DA techniques are based on the observation that it is possible to extract more information on a function rather than its mere values. The basic idea is to bring the treatment of functions and the operations on them to the computer environment in a similar way as the treatment of real numbers. Suppose two sufficiently regular functions f and g are given. In the framework of differential algebra, the computer operates on them using their Taylor series expansions, F and G respectively. Therefore, the transformation of real numbers in their floating point representation is now substituted by the extraction of the Taylor expansions of f and g. For each operation in the function space, an adjoint operation in the space of Taylor polynomials is defined, such that extracting the Taylor expansions of f and g and operating on them in the space of Taylor polynomials returns the same result as operating on f and g in the original space and then extracting the Taylor expansion of the resulting function.

The straightforward implementation of differential algebra allows to compute the Taylor coefficients of a function up to a specified order n, along with the function evaluation, with a fixed amount of effort. The Taylor coefficients of order n for sums and product of functions, as well as scalar products with reals, can be computed from those of summands and factors; therefore, the set of equivalence classes of functions can be endowed with well-defined operations, leading to an algebra, the so-called truncated power series algebra (Berz 1986, 1987). Similarly to the algorithms for floating point arithmetic, the algorithm for functions followed, including methods to perform composition of functions, to invert them, to solve nonlinear systems explicitly, and to treat common elementary functions (Berz 1991, 1999a). In addition to these algebraic operations, also the operations of differentiation and integration are introduced, which are invaluable for developing solvers for ODE and DAE. An operator satisfying the common sum and product rules of differentiation is called a derivation; and an algebra that also has a derivation is called a differential algebra. The differential algebra sketched in this section was implemented by M. Berz and K. Makino in the software COSY INFINITY (Berz and Makino 2006). We conclude the discussion by pointing out that the DA methods can be extended to include a rigorous treatment about remainder bounds (Makino 1998), which in the future may be used to make the arguments of this paper fully rigorous.

3.1 Solution of parametric implicit equations

As will be highlighted in Sect. 4, the evaluation of the constraint functions typical of MGA transfers involves the solution of implicit equations. These equations become parametric in case the Taylor expansion of the functions is of interest rather than their pointwise evaluation. DA techniques can be effectively used to identify the solution of parametric implicit equations in terms of Taylor polynomials, as described in Berz (1999b); Hoefkens (2001); Di Lizia et al. (2008), and here summarized for the sake of completeness.

Well-established numerical techniques (e.g., Newton's method) exist, which can effectively identify the solution of a classical implicit equation

$$f(x) = 0. \tag{1}$$

Suppose an explicit dependence on a parameter p can be highlighted in the previous function f, which leads to the parametric implicit equation

$$f(x, p) = 0. \tag{2}$$

Suppose the previous equation is to be solved, whose solution is represented by the function $x(p)$ returning the value of x solving (2) for any value of the parameter p. Thus, the dependence of the solution of the implicit equation on the parameter p is of interest. DA techniques can effectively handle the previous problem by identifying the function $x(p)$ in terms of its Taylor expansion with respect to the parameter p. The DA-based algorithm is presented in the followings for the solution of the scalar parametric implicit Eq. (2); the generalization to a system of parametric implicit equations is straightforward.

The solution of (2) is sought, where sufficient regularity is assumed to characterize the function f; i.e., $f \in \mathcal{C}^{n+1}$. This means that $x(p)$ satisfying

$$f(x(p), p) = 0 \tag{3}$$

is to be identified. The first step is to consider a reference value p^0 of the parameter p and to compute the value of the solution x^0 of the corresponding implicit equation by means of a classical numerical method; e.g., Newton's method. The variable x and the parameter p are then initialized as n-th order DA variables, i.e.,

$$\begin{aligned} [x] &= x^0 + \delta x \\ [p] &= p^0 + \delta p. \end{aligned} \tag{4}$$

A DA-based evaluation of the function f in (2) delivers the n-th order expansion of f with respect to x and p:

$$\delta f = \mathcal{M}_f(\delta x, \delta p), \tag{5}$$

where $\mathcal{M}_f$ denotes the Taylor map for f. Note that the map (5) is origin-preserving as x^0 is the solution of the implicit equation for the nominal value of the parameter p^0; thus, δf represents the deviation of f from its reference value $f^0 = 0$, resulting from deviations of x and p from x^0 and p^0, respectively. The map (5) is then augmented by introducing the map corresponding to the identity function on p (i.e., $\delta p = \mathcal{I}_p(\delta p)$) ending up with

$$\begin{pmatrix} \delta f \\ \delta p \end{pmatrix} = \begin{pmatrix} \mathcal{M}_f \\ \mathcal{I}_p \end{pmatrix} \begin{pmatrix} \delta x \\ \delta p \end{pmatrix}. \tag{6}$$

The n-th order map (6) is inverted using COSY INFINITY built-in tools, obtaining

$$\begin{pmatrix} \delta x \\ \delta p \end{pmatrix} = \begin{pmatrix} \mathcal{M}_f \\ \mathcal{I}_p \end{pmatrix}^{-1} \begin{pmatrix} \delta f \\ \delta p \end{pmatrix}. \tag{7}$$

As the goal is to compute the n-th order Taylor expansion of the solution manifold $x(p)$ of (2), the map (7) is evaluated for $\delta f = 0$

$$\begin{pmatrix} \delta x \\ \delta p \end{pmatrix} = \begin{pmatrix} \mathcal{M}_f \\ \mathcal{I}_p \end{pmatrix}^{-1} \begin{pmatrix} 0 \\ \delta p \end{pmatrix}. \tag{8}$$

The first row of map (8), which will be indicated as

$$\delta x = \mathcal{M}_{\delta f=0}(\delta p), \tag{9}$$

is the n-th order Taylor expansion of the solution manifold. For every value of p, the approximate solution of $f(x, p) = 0$ can be easily computed by evaluating the Taylor polynomial (9) at $\delta p = p - p^0$. Apparently, the solution obtained by means of the map (9) is a Taylor approximation of the exact solution of Eq. (2). The accuracy of the approximation depends on both the order of the Taylor expansion and the displacement δp from the reference value p^0. The performances of the previous algorithm will be assessed in Sect. 4 referring to the implicit equations involved in the evaluation of the constraint functions for MGA transfers.

4 Taylor expansion of the objective and constraint functions

The idea behind the introduction of DA techniques into GASP is substituting the pointwise evaluation of the constraint functions with a DA–based evaluation. However, expanding the constraint functions that typically characterize an MGA transfer is not trivial: a major issue can be identified, which is mainly related to the solution of implicit equations.

Three implicit equations appear in the evaluation process of the constraint and objective functions for the MGA transfers at hand. Two of them can be identified by analyzing simple planet-to-planet transfers. For the sake of clarity, consider the problem of transferring a spacecraft from Earth to Mars by means of two impulsive maneuvers (see Fig. 3). The typical objective function for this problem is the overall ΔV that can be evaluated by means of two design variables. A common choice is selecting the departure epoch from Earth, T_E, and the time of flight from Earth to Mars, t_{EM}, as design variables. Given T_E and t_{EM}, the arrival epoch at Mars, T_M, can be easily computed, and the position and velocity of Earth and Mars at both ends of the transfer are obtained through the evaluation of the planetary ephemerides. Then, given the initial and final positions, and the time of flight, the corresponding Lambert's problem is solved to compute the heliocentric initial velocity, $\boldsymbol{v}_1$, the spacecraft must be supplied with at Earth to reach Mars in the given time of flight, as well as the resulting heliocentric velocity at Mars, $\boldsymbol{v}_2$. The initial relative velocity of the spacecraft with respect to Earth, $\Delta \boldsymbol{V}_1$, and the final relative velocity with respect to Mars, $\Delta \boldsymbol{V}_2$, are readily computed. The optimization problem consists in minimizing

$$\Delta V = \|\Delta \boldsymbol{V}_1\| + \|\Delta \boldsymbol{V}_2\| = \Delta V_1 + \Delta V_2, \tag{10}$$

subject to the constraints

$$\begin{aligned} \Delta V_1 &\leq \Delta V_{1,\max} \\ \Delta V_2 &\leq \Delta V_{2,\max}\,. \end{aligned} \tag{11}$$

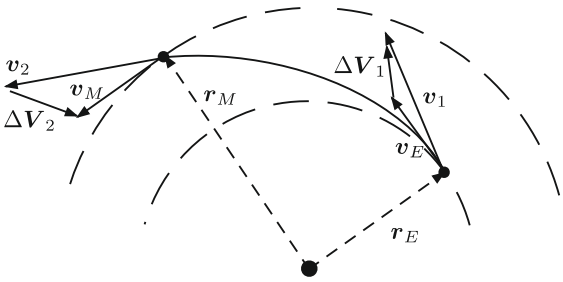

Fig. 3 A two-impulse Earth–Mars transfer

The evaluation of planetary ephemerides is required to compute the objective function (10) and the constraint functions (11). An analytical ephemeris model is used, which is based on fitting the orbital elements of the planets delivered by JPL ephemeris evaluations (Giorgini et al. 1998). A third order interpolation is selected to limit the interpolation error to the order of a few thousand km for the position and m/s for velocities over the time windows of interest, an accuracy compatible with the preliminary optimization problems at hand. In particular, the analytical model is able to supply the eccentricity of the planet orbit, e, and the mean anomaly of the planet, M, as a function of the input epoch. Then, the Kepler equation

$$f(E) = E - e\sin E - M = 0 \tag{12}$$

must be solved for the eccentric anomaly, E, which is necessary to evaluate the planet position and velocity.

Moreover, given the positions of Earth and Mars, and the time of flight between the two planets, the Lambert problem must be solved to obtain the initial and final heliocentric velocities of the spacecraft. In particular, it is necessary to find the solution of the Lagrange's equation for the time of flight, that concisely reads (see Battin 1987 for details)

$$f(x) = A(x) - t = 0, \tag{13}$$

where x is related to the semi–major axis of the resulting transfer orbit, A is a function depending on both x and some geometrical properties of the conic arc, and t is the transfer time. The solution is found via a secant method applied to the logarithm of Eq. (13) to improve the convergence rate of the numerical scheme. Once the solution is found, the initial and final heliocentric velocities of the spacecraft are computed via algebraic and transcendental functions.

The third implicit equation occurs only when a powered gravity assist appears. Within this model, the spacecraft can provide a tangential impulse at the pericenter of the incoming hyperbola (see Fig. 4), thus the planetocentric trajectory is made up by two arcs of hyperbola patched together. The angle α, usually referred to as bending angle, between the incoming and the outgoing asymptotic velocities, $\boldsymbol{v}_\infty^{in}$ and $\boldsymbol{v}_\infty^{out}$ respectively, is related to the pericenter radius via (Izzo et al. 2006)

$$f(r_p) = \arcsin\frac{a^-}{a^- + r_p} + \arcsin\frac{a^+}{a^+ + r_p} - \alpha = 0, \tag{14}$$

where $a^- = 1/(\boldsymbol{v}_\infty^{in} \cdot \boldsymbol{v}_\infty^{in})$ and $a^+ = 1/(\boldsymbol{v}_\infty^{out} \cdot \boldsymbol{v}_\infty^{out})$. Given the two heliocentric arcs to be connected by the powered gravity assist maneuver, the angle α can be easily computed through geometrical relations. The solution of the third implicit Eq. (14) delivers the pericenter radius of the planetocentric trajectory. The planetocentric velocities $\boldsymbol{v}_p^{in}$ and $\boldsymbol{v}_p^{out}$ at the pericenter, corresponding to the incoming and outgoing hyperbolic arcs respectively, are

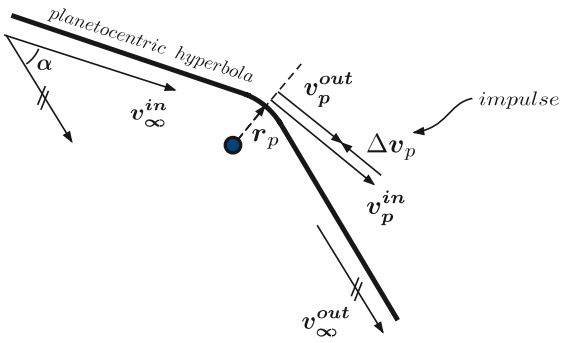

Fig. 4 Powered gravity assist

computed using $\boldsymbol{r}_p$, $\boldsymbol{v}_\infty^{in}$, and $\boldsymbol{v}_\infty^{out}$. Then, the required impulsive maneuver at the pericenter, $\Delta\boldsymbol{v}_p$, is the mere difference between $\boldsymbol{v}_p^{out}$ and $\boldsymbol{v}_p^{in}$.

If a pointwise evaluation of the objective and constraint functions is of interest, as in the standard implementation of GASP, a classical numerical method for the solution of implicit equations can be used. This is not possible when the Taylor expansion of the objective and constraint functions with respect to the optimization variables is of interest. Consider the evaluation of planetary ephemerides for explanation purposes. When dealing with the Taylor expansion of the ephemerides, the Kepler Eq. 12 cannot be solved for real values of the eccentric anomaly, but for its Taylor expansion with respect to the epoch. More specifically, suppose the expansion of the ephemerides of a planet about a reference epoch T^0 is sought. Once the epoch is initialized as DA variable (i.e., $[T] = T^0 + \delta T$) the evaluation of the analytical ephemeris model delivers the eccentricity e and the mean anomaly M as Taylor expansions with respect to the epoch,

$$\begin{aligned} e(\delta T) &= \mathcal{M}_e(\delta T) \\ M(\delta T) &= \mathcal{M}_M(\delta T). \end{aligned} \tag{15}$$

The next step is solving the Kepler equation to obtain the Taylor expansion of the solution E with respect to the parameter T. Indeed, the explicit dependence of e and M on T must be kept and Kepler's equation reads

$$f(E, \delta T) = E - e(\delta T) \sin E - M(\delta T) = 0. \tag{16}$$

The solution of this parametric implicit equation is attained in terms of the Taylor expansion $E(\delta T) = \mathcal{M}_E(\delta T)$ using the techniques illustrated in Sect. 3.1. Once $\mathcal{M}_E(\delta T)$ is available, the Taylor expansions of the planet position and velocity are readily obtained by carrying out the remaining algebra in the DA framework.

Clearly, the accuracy of the expansions depends both on the DA order and on the distance from the reference epoch; i.e., on the value of δT. Figures 5 and 6 display the accuracy referring to Mars' ephemerides. In particular, the reference epoch 1456 MJD2000 is selected. The Taylor expansions of Mars' position and velocity around the reference epoch are computed using differential algebra. The resulting polynomial maps are reported in Appendix, considering an interval of 40 days around the reference epoch. For each δT, the position and velocity of Mars are evaluated using both the Taylor expansions and the pointwise evaluations. Figures 5 and 6 report the error of the Taylor expansions with respect to the pointwise evaluations, in terms of the maximum norm of the difference vectors between the corresponding positions and velocities, respectively. The figures clearly show that, although the accuracy of the Taylor expansion decreases moving away from the reference date, it can be effectively

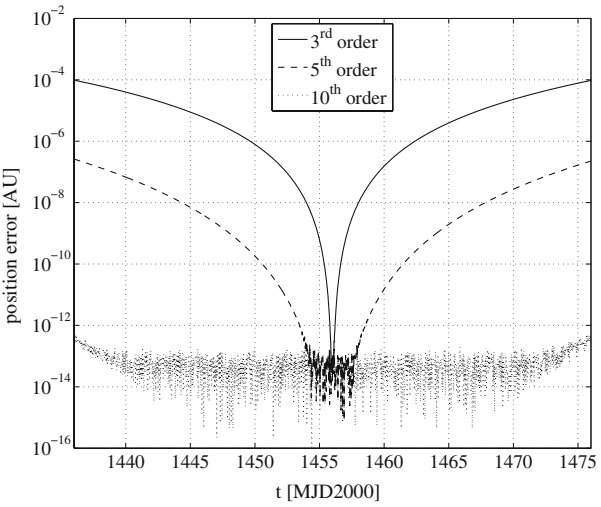

Fig. 5 Accuracy of the Taylor expansion of Mars position

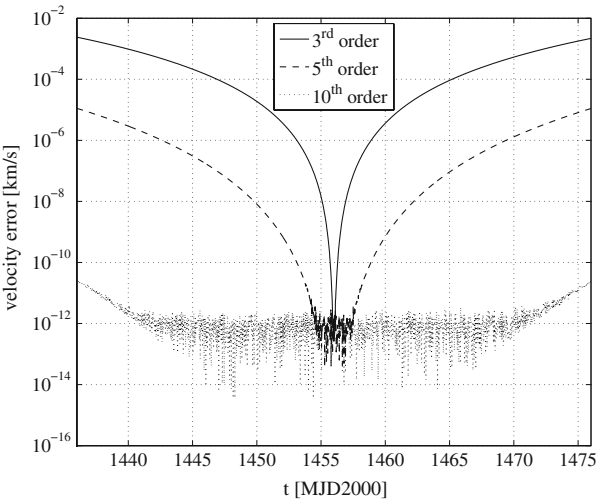

Fig. 6 Accuracy of the Taylor expansion of Mars velocity

kept to a suitable level by varying the expansion order. Note that, although the ephemerides are already expressed as polynomials, their DA evaluation is necessary to compute the Taylor expansion of the position and the velocity starting from orbital parameters.

5 Introduction of DA techniques into GASP

The complete extension of GASP algorithm is now possible. Two main difficulties arise when the attempt to introduce DA techniques into GASP is made. These difficulties will be referred to as *discontinuity* and *dependency* problems in the following subsections.

5.1 Discontinuity problem

The extension of GASP would be straightforward in the case of regular constraint and objective functions. Nevertheless, significant discontinuities characterize these functions in optimization problems involving MGA transfers, which are mainly related to geometrical considerations. To introduce the discontinuity problem, consider the following typical GASP-based pruning algorithm for the representative Earth-Mars transfer of Fig. 3:

1. *Subdivide the search space into boxes and put them in a list* $\mathcal{L}$
2. *While* $\mathcal{L} \neq \emptyset$*:*
   a. *take out a box* $[\boldsymbol{X}] = \{[T_E], [t_{EM}]\}$ *from* $\mathcal{L}$
   b. *initialize* T_E *and* t_{EM} *as DA variables and compute the Taylor expansion of* ΔV_1 *on* $[\boldsymbol{X}]$
   c. *bound the polynomial expansion of* ΔV_1 *on* $[\boldsymbol{X}]$*; i.e., estimate its minimum* $\underline{\Delta V_1}$ *and maximum* $\overline{\Delta V_1}$ *on* $[\boldsymbol{X}]$
   d. *if* $\underline{\Delta V_1} > \Delta V_{1,max} \Rightarrow$ *discard the current box* $[\boldsymbol{X}]$ *and go to step* a.
   e. *compute the Taylor expansion of* ΔV_2 *on* $[\boldsymbol{X}]$
   f. *bound the polynomial expansion of* ΔV_2 *on* $[\boldsymbol{X}]$*; i.e., estimate its minimum* $\underline{\Delta V_2}$ *and maximum* $\overline{\Delta V_2}$ *on* $[\boldsymbol{X}]$
   g. *if* $\underline{\Delta V_2} > \Delta V_{2,max} \Rightarrow$ *discard the current box* $[\boldsymbol{X}]$ *and go to step* a.
   h. *keep* $[\boldsymbol{X}]$ *in a list of feasible boxes*

It is worth mentioning that bounding the Taylor expansions, as required in steps 2.c. and 2.f. of the previous algorithm, is not a trivial task. Although a quadratic estimation process is used in the current version of the DA-based GASP (see Sect. 6.1), the basic tool used for the example reported here is the linear dominated bounder described in Makino (1998).

The previous algorithm is implemented in COSY INFINITY. In particular, a search space of 5000 days on the departure epoch ($T_E \in [1000, 6000]$ MJD2000) and 500 days on the transfer time ($t_{EM} \in [100, 600]$) is selected. Figure 7 illustrates the ΔV landscape over the defined search space. Quasi-periodicities related to the synodic period of the Earth–Mars system (about 2.14 years) can be identified (see Di Lizia and Radice 2004 for details). Figure 8 reports instead the search space remaining after imposing the fulfillment of two pruning constraints

$$\begin{aligned} \Delta V_1 &\leq 5\,\text{km/s} \\ \Delta V_2 &\leq 5\,\text{km/s}. \end{aligned} \tag{17}$$

The DA-based pruning algorithm illustrated above is now applied to this relatively simple problem. In particular, the search space is uniformly subdivided in boxes of size 50 days on each design variable. The pruning process is then performed using the constraints (17). The boxes remaining after pruning are reported in Fig. 9 on the pruned search space of Fig. 8, which is aimed to be enclosed by the algorithm. Figure 9 clearly shows that the accuracy of the attained enclosure is not satisfactory. Specifically, even if the remaining boxes enclose the desired portion of the search space, some undesired boxes remain after pruning, which should have been pruned away. To better understand this behavior, compare Fig. 9 with Fig. 7. As can be clearly recognized, these unsought remaining boxes tend to lie on lines over

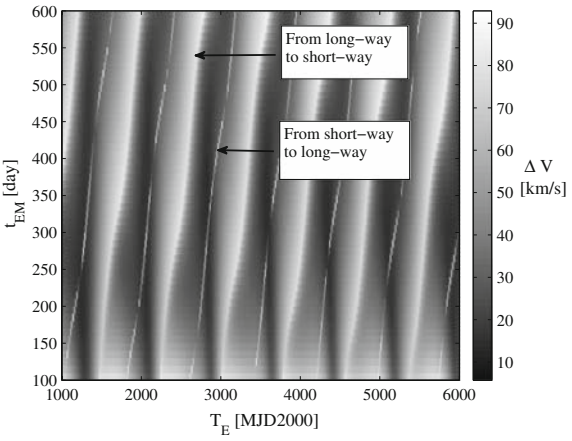

Fig. 7 ΔV landscape and discontinuities for the Earth–Mars transfer

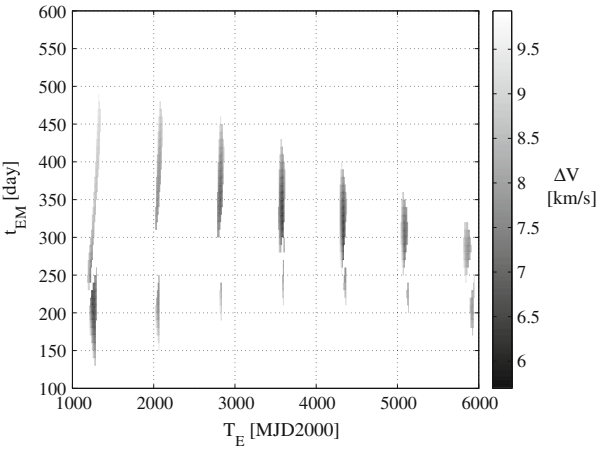

Fig. 8 ΔV landscape for the Earth–Mars transfer after pruning

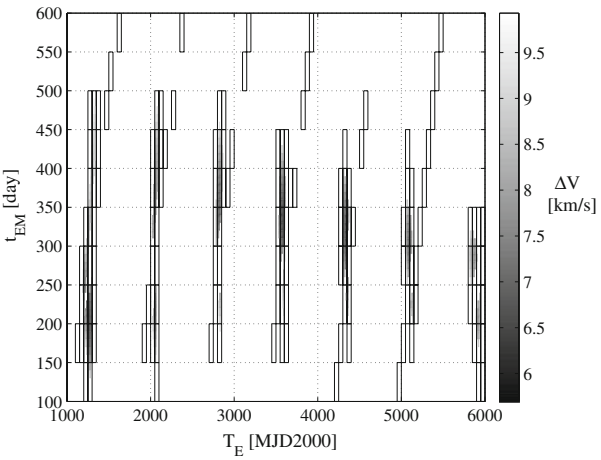

Fig. 9 Enclosure of the pruned search space for the Earth–Mars transfer

the search space, which can be related to discontinuities of this problem. Such discontinuities correspond to the so-called transitions from the "short–way" to the "long–way" solutions of the Lambert's problem (and vice versa) when crossing regions of the search space where the transfer occur on an orbital plane that is perpendicular to the ecliptic. This regions are actually lines over the design space (see Fig. 7). Consequently, they differ from the well-know singularities of the same problem corresponding to both a 180° and a 360° transfer, which are due to the ambiguity in the selection of the transfer plane. More specifically, as better detailed by Kemble (2006); Bernelli-Zazzera et al. (2006), the solution of the Lambert's problem asks for transfer planes of higher and higher inclination as one gets close to these lines in the design space. In the framework of a planet-to-planet transfer, given the low inclination of the planetary orbits, this entails a steep increase of the ΔV. This process continues until a transfer plane perpendicular to the ecliptic is achieved. Here, northerly transfers switch to southerly transfers (and vice versa) to keep dealing with prograde orbits. Switching from northerly transfers to southerly transfers implies switching from short–way to long–way solutions or from long–way to short–way solutions. Corresponding to these transitions, a jump on the ΔV occurs. This jump is very small in general (especially referring to transitions from the short–way to the long–way solution) due to the low inclination of the planetary orbits.

It is well known that Taylor polynomial expansions fail when discontinuities on the processed function occur. This can be deemed as the cause of the presence of undesired boxes after pruning: Taylor expansions within boxes lying on the discontinuity do not accurately approximate the constraint functions; consequently bounds of the corresponding ranges are wrongly estimated, and the boxes tend to be kept in the list of admissible boxes.

Extensive work has been devoted to overcome the discontinuity problem, and to improve the accuracy of the enclosure of the pruned search space (see Bernelli-Zazzera et al. 2006 for details). The idea for the adopted solution came from the observation that the unfavorable discontinuity lines (i.e., the lines close to good local minima) correspond to the transition from the short–way to the long–way solution of the Lambert's problem. These discontinuity lines vanish if a planar planetary model is used instead of the actual three-dimensional model associated to the ephemeris evaluator: the orbital plane of the connecting Lambert's arc is uniquely determined as coinciding with the ecliptic, and the transition from the short–way to the long–way solution is continuous.

A major observation can be stated, which is the main driver for the following decisions. A systematic analysis of the difference between the ΔV in the three-dimensional, ΔV_{3D}, and the planar, ΔV_{2D}, planetary models over the entire search space was performed. It turns out that $\Delta V_{3D} \geq \Delta V_{2D}$ on the whole search space. Consequently, if the pruning process is performed in the planar planetary model, no branches of the feasible domain in the real three-dimensional model are lost. In other words, the boxes remaining after the pruning process performed on the planar model include the feasible domain of the real three-dimensional model.

Given the previous considerations, a planar planetary model is adopted in the DA-based GASP algorithm to perform the pruning process. No mathematical proof is supplied about the validity of this conservative hypothesis for a general transfer. The low inclination of all planetary orbits, and geometrical considerations, lead to the decision of conjecturing its validity for interplanetary transfers in the solar system. Although more rigorous mathematical considerations should be sought in future works, the fairness of the hypothesis is confirmed by an extensive test campaign (Bernelli-Zazzera et al. 2006).

It is worth stressing that the use of the planar model is not strictly made to approximate the real three-dimensional model, but rather to "filter" the three-dimensional model in such a way that

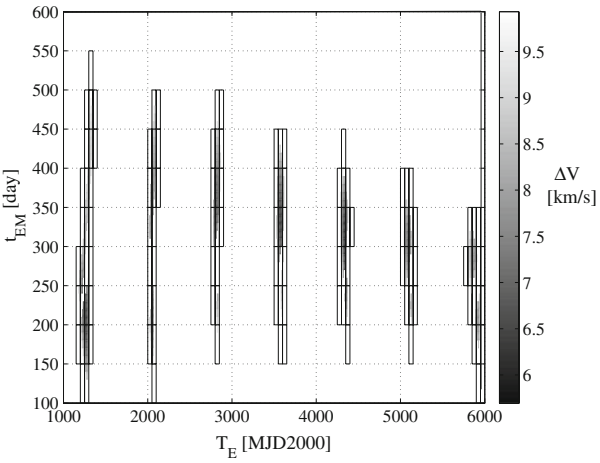

Fig. 10 Enclosure of the pruned search space for the Earth–Mars transfer using the planar model

– the unsought boxes remaining after the pruning process on the discontinuity lines are eliminated;
– no branches of the feasible domain of the real three-dimensional model are lost.

We anticipate that the previous approximation is used within the pruning process only, whereas the subsequent optimization processes in the remaining boxes are performed within the actual three-dimensional planetary model.

As a further proof of the validity of the approximation, the performances of the resulting pruning algorithm on the Earth–Mars transfer problem are analyzed in Fig. 10. The boxes remaining after the pruning process carried out in the planar model sharply enclose the pruned search space of the three-dimensional model. A plain improvement in enclosure accuracy can be detected by comparing Fig. 10 with Fig. 9.

5.2 Dependency problem

The considerations reported in Sect. 5.1 are based on analyses performed within the framework of a planet-to-planet transfer, where the departure epoch and the transfer time are selected as design variables. However, an alternative problem formulation is preferable. In particular, substituting the arrival epoch in place of the transfer time in the set of design variables has already shown important advantages from a computational point of view (Izzo et al. 2006), as it significantly reduces the number of ephemeris evaluations required by the pruning algorithm. Together with the particular mathematical model adopted for the design of MGA transfers, this allows the whole process to gain a polynomial complexity. Further reasons of selecting this second formulation can be outlined, which are important alike for the DA-based GASP, especially if actual MGA transfers are studied.

Consider the scheme of an Earth–Mars–Jupiter transfer, reported in Fig. 11. The set of design variables usually selected for this MGA transfer is composed of the departure epoch from Earth, T_E, the transfer time from Earth to Mars, t_{EM}, and the transfer time from Mars to Jupiter, t_{MJ}. For the sake of clarity, this formulation is referred to as "relative times formulation" in the followings.

The evaluation of the overall ΔV starts in general from the analysis of the first arc connecting Earth to Mars. Suppose the relative times formulation is being used. Thus, referring to Fig. 12, the quantities related to the first arc are characterized in the (T_E, t_{EM})-plane. As

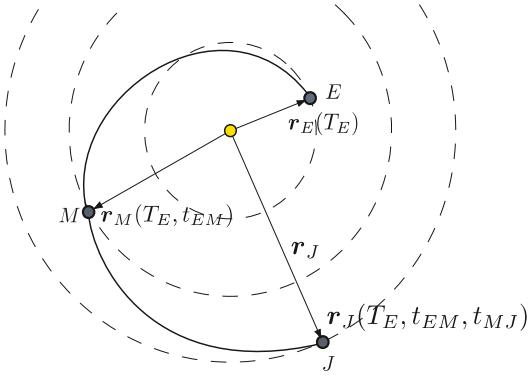

Fig. 11 Scheme of an Earth–Mars–Jupiter transfer

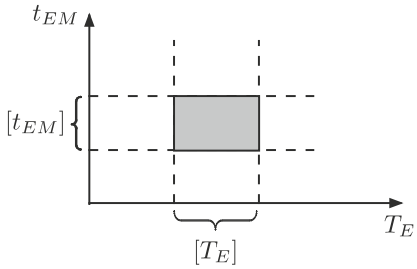

Fig. 12 Design space for the first arc of the Earth–Mars–Jupiter transfer

both T_E and t_{EM} are design variables, in the framework of the DA-based GASP, a box is readily identified by the DA representation of both variables, and the computation goes on as depicted in the previous sections. Suppose now the first arc has been processed, and the second arc from Mars to Jupiter is of interest. The quantities associated to the second arc are characterized in the (T_M, t_{MJ})-plane, where T_M is the arrival epoch at Mars. However, T_M is not a design variable in the relative times formulation, and it is computed as $T_M = T_E + t_{EM}$. Even if t_{MJ} is a design variable, the size of the corresponding interval on T_M is the sum of the box size on T_E and t_{EM} in the DA-based GASP. The previous considerations can be easily extended to MGA transfers involving more than three planets: the box size on the departure epoch from each planet increases along the transfer. This effect is strongly related to the dependencies associated to the relative times formulation.

The problem dependencies are highlighted in Fig. 11. Focusing on the dependence of the planetary ephemerides on the design variables, the position of Earth, $\boldsymbol{r}_E$, depends only on the departure epoch T_E. The position of Mars, $\boldsymbol{r}_M$, is evaluated using the epoch at Mars T_M. Consequently, $\boldsymbol{r}_M$ will depend on the two variables T_E and t_{EM}. Similarly, the dependence of the position of Jupiter on the three variables T_E, t_{EM}, and t_{EJ} is highlighted. Thus, in an MGA transfer involving n planets, the position of the i-th planet will depend on the departure epoch from Earth, and all the transfer times associated to the prior $i-1$ connecting arcs. Therefore, the dimensionality of the dependency increases along the transfer, reaching its maximum corresponding to the last connecting arc, where quantities will depend on all n variables. Similar arguments hold for the associated ΔV, on which inequality constraints are usually set.

The previous dependency problems can be overcome using the alternative strategy of Myatt et al. (2004). In particular, the departure epoch from Earth is kept within the set of design variables, whereas the transfer times are replaced by the epoch at each remaining

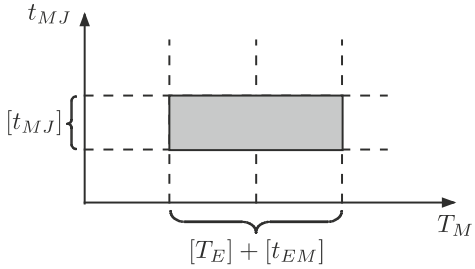

Fig. 13 Design space for the second arc of the Earth–Mars–Jupiter transfer

planet of the MGA sequence. Referring again to the Earth–Mars–Jupiter transfer, the new set of variables will include the epochs at Earth, T_E, Mars, T_M, and Jupiter, T_J. In contrast to the relative times formulation, the new formulation is referred to as the "absolute times formulation" in the followings.

A review of the previous analyses will be of help to gain a valuable insight on the advantages of the new formulation. Consider again Figs. 12 and 13. Using the absolute times formulation allows both arcs to be characterized within planes that are directly defined by design variables. Thus, no increase in box size occurs along the transfer. Referring instead to Fig. 11, the planetary ephemerides will depend on the epoch of the planet, which is now included in the set of design variables. If the ΔV associated to the whole transfer are of interest (which is the case in the pruning process of GASP), it can be easily shown that the maximum dimensionality of the dependency corresponds to the ΔV of the powered gravity assist maneuvers, which will depend on three design variables. The outcome of the previous analysis led to the decision of adopting the absolute times formulation as the baseline approach in the DA-based GASP.

6 Test cases

In this section, relevant test cases are addressed to assess the performances of the DA-based GASP algorithm. After the pruning, an optimization process must occur within the remaining boxes to serve the purpose of optimizing the overall ΔV and identifying optimal transfer solutions. Consequently, before illustrating the results of the test phase, Sect. 6.1 describes the philosophy adopted for this optimization process. The performances of the algorithm on several test cases are then reported, ordered by increasing complexity.

For each test, the problem is first defined. The search space is identified by indicating lower and upper bounds on each variable. Referring to the box-wise approach of the DA-based GASP, the size of the sampling boxes corresponding to each variable is reported. The cutoff values for the departure and arrival ΔV, as well as for the corrective ΔV at each powered gravity assist, are indicated. Concerning the minimum allowed pericenter radii for the gravity assist maneuvers, a common rule has been adopted for all the planets: given the mean radius of a planet P, R_P, the corresponding minimum allowed pericenter radius is set to $1.05\,R_P$.

Then, the results of the pruning process are reported in terms of the total number of boxes, the number of feasible boxes remaining after pruning, and the CPU time required by the pruning process. It is worth observing that the total number of boxes is meant to give an idea on the dimension of the search space, and it is different from the number of the boxes processed, thanks to the forward and backward constraint propagation (see Sect. 2). The computational

time is relative to a PC, 1.9 GHz CPU, 512 Mb RAM. As far as the optimization process is concerned, the best solution identified and the associated ΔV are reported.

6.1 Optimization process

The outcome of the pruning process carried out by the DA-based GASP is a list of boxes, all fulfilling the requirement that at least a portion of them satisfies the feasibility conditions related to the constraining ΔV values and the minimum allowed pericenter values. An optimization process is then necessary to locate the minimum of the objective function, which is the purpose of the original optimization problem.

Before describing the details of the optimization process, some notes are given about the polynomial bounders adopted in the pruning process. In all the previous examples, the linear dominated bounder (LDB) algorithm is used to estimate the range of the constraint functions over each box. The LDB algorithm is introduced in the framework of Taylor models (Makino 1998; Makino and Berz 2005; Berz et al. 2006) and it is based on the observation that the dominating part of the total bounds of a polynomial are expected to come from the linear part. This algorithm is capable of producing validated bounds for polynomials of any order. Unfortunately, range overestimation problems appear when LDB is used for complex MGA transfers, which led to the decision of implementing a non-validated quadratic bounder in the current version of the DA-based GASP (Bernelli-Zazzera et al. 2006). The non–validated bounder makes use of the quadratic part of the Taylor expansion to get estimates of the minimum of a function over each box. More specifically, if the resulting quadratic polynomial is positive definite, its minimum is easily estimated by locating the zero–gradient point, and checking its inclusion within the box. Only linear information is used instead in the case of lack of positive definition properties. An evident drawback is that, in contrast to the validated LDB, the non-validated quadratic bounder could underestimate the exact enclosure. However, an extensive test campaign confirmed the validity of the introduced approximations (Bernelli-Zazzera et al. 2006). Moreover, thanks to the second order information, besides the minimum of the function within each box, estimates for its location are returned.

It is worth pointing out that, if the non-validated quadratic bounder is used, there are no advantages and reasons to use expansion orders greater than two. Consequently, second order expansions are used in all the test cases for the DA-based pruning process. This choice necessarily constrains the size of the boxes, which must be selected in such a way to prevent excessive accuracy loss. Furthermore, even in the case of smooth and regular functions, clustered minima may occur, which further affects the maximum allowed box size. Therefore, a test campaign was carried out to support the proper selection of the box size. More specifically, the DA–based GASP algorithm was applied to test cases available in the literature using second order expansions. Estimates for the maximum box size to be used in order to avoid losing the identification of the known best solutions were obtained. The resulting estimates turned out to assure in any case a reduced computational effort with respect to the classical implementation of GASP. The results of this analysis supplied the heuristics for the selection of the box size in other applications.

It is now possible to detail the philosophy adopted for the optimization process, which mainly relies on multiple runs of a local optimizer, based on the following steps:

1. the aforementioned non-validated bounding process is used to estimate the minimum value of the objective function of the planar model, as well as its location, within each box;

2. the boxes are sorted based on the minimum objective function values estimated in step 1;
3. a number of these boxes are properly selected;
4. starting from the estimated location of the minimum, a local optimization process is run within each selected box by minimizing the overall ΔV associated to the actual three-dimensional transfer problem.

The previous optimization philosophy deserves some comments. Different models for the constraint and objective functions evaluation are implemented in the two main phases of the previous algorithm; i.e., search space pruning and total ΔV optimization. In particular, the planar planetary model is used within the search space pruning phase only. This decision relies on the conservative hypothesis pertaining the planetary model depicted in Sect. 5.1. This approximation is abandoned in the subsequent optimization process of step 4, where the actual three-dimensional planetary model, and the iterative Newton method are used to evaluate the planetary ephemerides and to compute the solutions of the implicit equations.

Moreover, the box selection phase (step 3) is based on the following heuristics. Suppose the overall objective function range is available, which is computed on all the minima identified within each box in step 1. Only the boxes with an estimated function value within the lowest 5 percentile of all the registered function values are selected. The 5% value is purely based on the experience gained during extensive test campaigns. The parameter is anyway kept settable by the user.

The local optimization runs involved in step 4 are carried out within each box. This means that the identified local minima are interior to the feasible boxes, as well as the finally estimated global minimum. Moreover, the objective function used in the optimization phase is the overall ΔV associated to the actual three-dimensional transfer problem. Consequently, based on the conjecture in Sect. 5.1, local minima of the three-dimensional transfer problem are identified, as the boxes remaining after the pruning process performed on the planar planetary model enclose the feasible domain of the real three-dimensional planetary model.

The local optimization runs are carried out using sequential quadratic programming and they require a first guess solution. Instead of using random first guesses, the information available from the planar model adopted in the pruning process are used to identify good first guesses for the local optimization runs, based on the heuristics that the planar model is an acceptable approximation of the three-dimensional model for this purpose. More specifically, within each box, the estimated location of the minimum of the objective function obtained in the planar planetary model is used as first guess solution. It is worth observing that, based on this procedure, only one local minimum is identified within each box. Consequently, good local minima are likely to be lost if more than one local minimum is enclosed within a box. This constrains the size of the boxes to be used in the pruning process.

6.2 Earth-Mars transfer

The first test case is the Earth–Mars transfer. The search space is defined in Table 1. It is worth observing that bounds on the departure epoch from Earth, T_E, and on the transfer time from Earth to Mars, t_{EM}, are given. Consequently, the search space definition is made within the relative times formulation. However, as stated in Sect. 5.2, pruning is carried out in the absolute times formulation. This observation holds for all the following test cases. The box size along each epoch is indicated in the fifth column. The cutoff values for the maximum allowed departure and arrival ΔV are reported in the sixth column. A further constraint is imposed on the maximum allowed overall ΔV, which is reported within round brackets on the head row in the same column.

Table 1 Search space and best solution identified for the EM transfer

Planet	Variable	Lower bound (days)	Upper bound (days)	Size (days)	Cutoff (10) (km/s)	Solution (days)
E	T_E	1000	6000	50	5	3573.188
M	t_{EM}	100	600	50	5	324.047

The main results pertaining the performances of the DA-based GASP are:

- Total number of boxes: 1000
- Feasible boxes: 64 (6.4%)
- CPU time: 0.220 s
- Best identified ΔV: 5.6673 km/s

The reported value of the best ΔV refers to the results of the optimization process described in Sect. 6.1, which follows the DA-based pruning process. The last column of Table 1 lists the values of the design variables corresponding to the best solution identified.

6.3 Earth–Venus–Mars transfer

One planet is added to the sequence of planets involved in the transfer, where a powered gravity assist maneuver is performed. In particular, an Earth–Venus–Mars transfer is investigated. The search space is defined in Table 2. The cutoff values at Earth and Mars are still related to the departure and arrival ΔV, whereas the cutoff value of 2 km/s at Venus now refers to the maximum allowed corrective ΔV at the pericenter of the corresponding hyperbolic trajectory, as provided by the powered gravity assist model.

The main performance parameters are:

- Total number of boxes: 14400
- Feasible boxes: 165 (1.1%)
- CPU time: 1.8321 s
- Best identified ΔV: 8.5226 km/s

The last column of Table 2 reports the optimal solution identified at the end of the optimization processes. A two-dimensional plot of the corresponding trajectory can be found in Fig. 14.

6.4 Cassini-like transfer

This section is devoted to an MGA transfer problem which has already been analyzed in the past (Izzo et al. 2006; Di Lizia and Radice 2004). Saturn is set as the target planet, which is

Table 2 Search space and best identified solution for the EVM transfer

Planet	Variable	Lower bound (days)	Upper bound (days)	Size (days)	Cutoff (12) (km/s)	Solution (days)
E	T_E	1000	6000	50	5	5611.480
V	t_{EV}	100	500	50	2	157.603
M	t_{VM}	100	1000	50	5	255.596

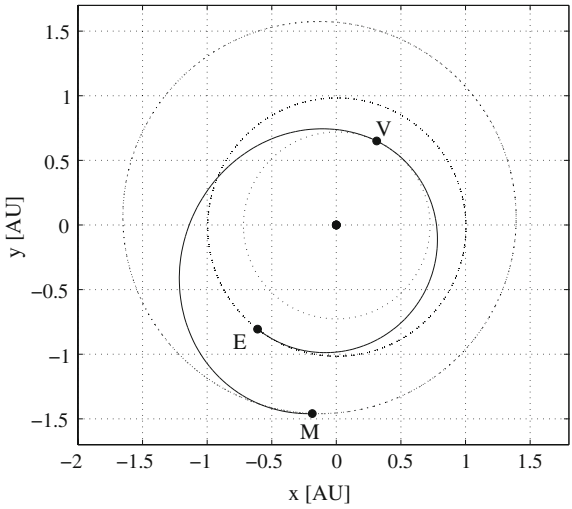

Fig. 14 Trajectory of the best EVM transfer

reached after four gravity assists. Thus, the overall transfer involves six planets, so leading to a six-dimensional optimization problem. The sequence is fixed to Earth–Venus–Venus–Earth–Jupiter–Saturn (EVVEJS), which can be evidently recognized to be the sequence of the Cassini mission (Peralta and Smith 1993), except no deep space maneuvers are allowed.

Before presenting the results for this test case, some notes must be reported about a further necessary expedient which has to be added in the case of MGA transfers where resonances might play an important role in the optimization, as in the EVVEJS transfer case. The discontinuity problem is solved by adopting a planar planetary model. Nevertheless, this strategy is not able to solve the same problem for the transition from the long–way to the short–way solution. The occurrence of this discontinuity is particularly undesirable in arcs where resonance conditions are known to improve the overall transfer performances, such as the Venus–Venus arc in the EVVEJS sequence. An expedient is introduced to overcome the previous difficulty, which is based on the observation that, in a planet-to-planet transfer involving only one planet, the discontinuity disappears if multi-revolution solutions for the Lambert's problem are used (Di Lizia 2008). In particular, given a box to be processed, if the enclosed transfer times include resonance conditions, the multi–revolution solution is allowed. In this manner, the EVVEJS test case can be effectively managed by the DA-based GASP, as illustrated in the followings.

The search space for the optimization problem is set as defined in Table 3. A maximum value of 12 km/s is used for the overall ΔV. The main results pertaining the performances of the algorithm are listed below:

– Total number of boxes: 32768000
– Feasible boxes: 1085 (0.003%)
– CPU time: 1.93 s
– Best identified ΔV: 4.9307 km/s

Note that the best identified ΔV refers to the final insertion of the spacecraft into an orbit around Saturn of eccentricity 0.98 and periapsis 108950 km, as considered in Izzo et al. (2006). For the sake of clarity, it is worth observing again that the total number of boxes is different from the number of boxes that must be processed during pruning. Thanks to the forward and backward constraint propagation, the latter is significantly lower then the

Table 3 Search space and best solution for the EVVEJS transfer

Planet	Variable	Lower bound (days)	Upper bound (days)	Size (days)	Cutoff (12) (km/s)	Solution (days)
E	T_E	−1000	0	50	4	−790.2077
V	t_{EV}	10	410	25	2	158.0403
V	t_{VV}	100	500	25	2	449.3858
E	t_{VE}	10	410	25	2	55.1819
J	t_{EJ}	400	2000	200	2	1019.7660
S	t_{JS}	1000	6000	200	6	4543.5110

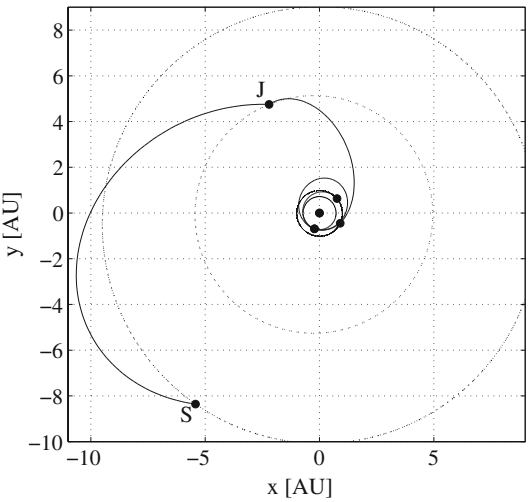

Fig. 15 Trajectory of the best EVVEJS transfer

former. Specifically for the problem at hand, the actual number of boxes processed turns out to be 4065.

Figure 15 reports a two-dimensional plot of the trajectory corresponding to the best identified solution, whose solution vector is listed in Table 3. The occurrence of a resonance at Venus can be verified in Fig. 16, which gives a detail of the whole transfer. The identified objective function value agrees with the known best one (http://www.esa.int/gsp/ACT/inf/op/globopt/evvejs.htm accessed on 7/7/2009).

7 Conclusions

This work investigated the benefits that DA techniques can bring to the pruning of the search space of a specific class of MGA transfers. More specifically, differential algebra was introduced to substitute the pointwise evaluation of objective function and constraints used in GASP with their Taylor expansions over sampling boxes. A 2D version of the MGA transfer modeling used in GASP was adopted. Significant work was devoted to address the discontinuity and dependency problems. The solution to the discontinuity problem was the use of a planar planetary model for the solar system, which was conjectured to be a conservative hypothesis for the analyzed transfers. The validity of this approach, limited to planetary

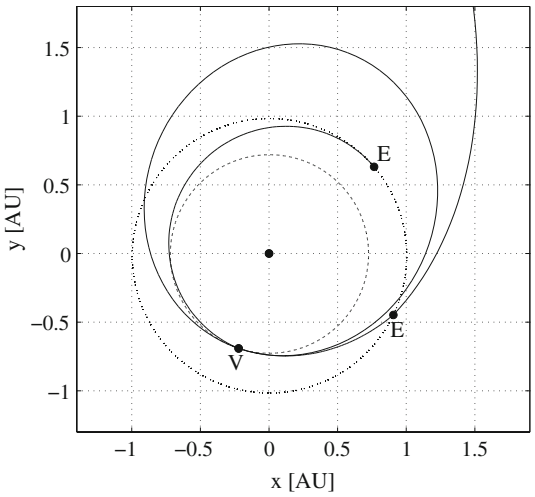

Fig. 16 EVVEJS transfer: detail of Fig. 15

transfers, was shown by the optimal solutions found running a sequential quadratic programming algorithm on the feasible domain.

The resulting DA-based GASP can handle wide sampling grids, ranging from 50 up to 200 days. Thus, as the computational effort for a second order DA evaluation is on average 20% greater than for its pointwise counterpart, a more computationally efficient pruning algorithm is obtained. Furthermore, the additional nuisance of estimating the Lipshitzian tolerance is avoided at the price of selecting a box size compatible with the expansion order. The test cases showed that

1. the pruning process is fast;
2. regions containing known optimal solutions are kept in the feasible domain;
3. a second order Taylor expansion is appropriate for both estimating the range of the objective function and constraints, and for obtaining good first guess solutions for the subsequent optimization process;

thus proving the effectiveness and the efficiency of the DA-based GASP.

The favorable results obtained also suggest to study the use of verified Taylor model based methods, which in addition to the polynomial approximations obtained with DA also provide rigorous bounds for the accuracy with which the polynomials represent the function over the local domain of interest. This may represent a viable approach towards the eventual development of fully rigorous optimization tools eventually for the pruning and optimization problem.

Acknowledgments This research has been carried out under European Space Agency(ESA)/Ariadna scheme, contract number: 20271/06/NL/HI. The authors would like to acknowledge the support of Tamás Vinkó and Dario Izzo from the Advanced Concept Team of ESA. Moreover, the authors are indebted to Kyoko Makino for all her support and help.

Appendix

The polynomial maps resulting from the application of the algorithm for the Taylor expansion of the solution of parametric implicit equations to the evaluation of planetary ephemerides

r_x [AU]		r_y [AU]		r_z [AU]	
COEFFICIENT	EXPONENT	COEFFICIENT	EXPONENT	COEFFICIENT	EXPONENT
0.9738329507571694	0	1.099506478391541	0	-0.9266849660391702E-03	0
-0.1988798644119760	1	0.2094385320182159	1	0.9274449212580083E-02	1
-0.1819229419906598E-01	2	-0.2053934734202566E-01	2	0.1731648672053160E-04	2
0.1546964348858368E-02	3	-0.9557735495179728E-03	3	-0.5804033450867999E-04	3
0.2471398672024257E-04	4	0.9665526115527965E-04	4	0.1415764649290540E-05	4
-0.5300282535152253E-05	5	-0.1048090239315998E-05	5	0.1083624047135448E-06	5
0.2042278294266370E-06	6	-0.2439243475129716E-06	6	-0.1012727829134618E-07	6
0.7518486511117514E-08	7	0.1839884777439683E-07	7	0.2003301909863849E-09	7
-0.1268281031785555E-08	8	-0.1164851727376397E-09	8	0.2874195393096650E-10	8
0.4524767746777855E-10	9	-0.6986097539252299E-10	9	-0.2574915925467360E-11	9
0.2725058616222821E-11	10	0.4841629105965710E-11	10	0.3436162201645452E-13	10

Fig. 17 10th order expansion of Mars position: polynomial maps corresponding to each component of the position vector

are reported here. More specifically, the Taylor expansions of Mars' ephemerides analyzed in Fig. 5 are presented. The epoch is first initialized as a DA variable: $[T] = T^0 + \delta T$, where T^0 is the reference epoch for the expansions. An analytical ephemeris model is then used to evaluate the eccentricity e and the mean anomaly M as Taylor expansions with respect to the epoch; i.e., $e(\delta T) = \mathcal{M}_e(\delta T)$, and $M(\delta T) = \mathcal{M}_M(\delta T)$. The Kepler equation is then solved in parametric form to attain the resulting Taylor expansion of the eccentric anomaly with respect to the epoch; i.e., $E(\delta T) = \mathcal{M}_E(\delta T)$. The identification of $\mathcal{M}_E(\delta T)$ relies on the use of the algorithm for the expansion of the solution of parametric implicit equations presented in Sect. 3.1. Once $\mathcal{M}_E(\delta T)$ is available, the Taylor expansions of the planet position and velocity with respect to the epoch,

$$\begin{aligned} \boldsymbol{r}(\delta T) &= \mathcal{M}_{\boldsymbol{r}}(\delta T) \\ \boldsymbol{v}(\delta T) &= \mathcal{M}_{\boldsymbol{v}}(\delta T), \end{aligned} \tag{18}$$

are readily obtained by means of mere algebraic manipulations.

Referring to the analysis performed in Fig. 5, the resulting 10-th order Taylor polynomials for each component of Mars' position are reported in Fig. 17. For each polynomial, the first column lists the coefficients of the Taylor expansions, whereas the second column shows the corresponding order. As the polynomials are monovariate expansions, the order coincides with the associated exponent for the expansion variable T. The polynomials reported in the figure refer to the maps

$$\begin{aligned} \boldsymbol{r}(\delta \tilde{T}) &= \mathcal{M}_{\boldsymbol{r}}(\delta \tilde{T}) \\ \boldsymbol{v}(\delta \tilde{T}) &= \mathcal{M}_{\boldsymbol{v}}(\delta \tilde{T}), \end{aligned} \tag{19}$$

with $\tilde{T} = T/(w/2)$, where w is the amplitude of the interval of epochs analyzed in Fig. 5; i.e., $w = 40$ days. The variable $\tilde{T}$ is introduced to suitably rescale the resulting polynomials, so avoiding possible numerical problems associated to the representation of the coefficients in the computer environment.

References

Battin, R.H.: An Introduction to the Mathematics and Methods of Astrodynamics, Second Printing. AIAA Education Series, Providence (1987)

Bernelli-Zazzera, F., Berz, M., Lavagna, M., Armellin, R., Di Lizia, P., and Topputo, F.: Global trajectory optimisation: can we prune the solution space when considering deep space maneuvers?. Final Report, Ariadna id: 06/4101, Contract No. 2007/06/NL/HI (2006)
Berz, M.: The new method of TPSA algebra for the description of beam dynamics to high orders. Technical Report AT-6:ATN-86-16, Los Alamos National Laboratory (1986)
Berz, M.: The method of power series tracking for the mathematical description of beam dynamics. Nucl. Instrum. Methods **A258**, 431 (1987)
Berz, M.: High-Order computation and normal form analysis of repetitive systems. Phys. Part. Accelerators **AIP 249**, 456 (1991)
Berz, M.: Differential algebraic techniques. In: Tigner, M., Chao, A. (eds.) Handbook of Accelerator Physics and Engineering, World Scientific, Singapore (1999a)
Berz, M.: Modern Map Methods in Particle Beam Physics. Academic Press, San Diego (1999b)
Berz, M., Makino, K.: COSY INFINITY version 9 reference manual, MSU Report MSUHEP-060803, Michigan State University, East Lansing, MI 48824 (2006)
Berz, M., Makino, K., Kim, Y.-K.: Long-Term Stability of the Tevatron by Validated Global Optimization. Nucl. Instrum. Methods **558**, 1–10 (2006)
Betts, J.T.: Practical Methods for Optimal Control Using Nonlinear Programming. Society for Industrial and Applied Mathematics, Philadelphia PA (2001)
Di Lizia, P.: Robust space trajectory and space system design using differential algebra. Dissertation, Politecnico di Milano (2008)
Di Lizia, P., Radice, G.: Advanced global optimisation for mission analysis and design. Final Report, Ariadna id: 03/4101, Contract No. 18139/04/NL/MV (2004)
Di Lizia, P., Armellin, R., Lavagna, M.: Application of high order expansions of two-point boundary value problems to astrodynamics. Celestial Mechanica Dynamical Astron. **102**, 355–375 (2008)
Giorgini, J.D., Yeomans, D.K., Chamberlin, A.B., Chodas, P.W., Jacobson, R.A., Keesey, M.S., Lieske, J.H., Ostro, S.J., Standish, E.M., Wimberly, R.N.: Horizons, JPL's On-Line Solar System Data and Ephemeris Computation Service. User's guide (1998)
Hoefkens, J.: Rigorous numerical analysis with high-order Taylor models. Dissertation, MSU (2001)
Ingberg, L.: Simulated annealing: practice versus theory. Math. Comput. Model. **18**, 29–57 (1993)
Izzo, D., Becerra, V., Myatt, D., Nasuto, S., Bishop, J.: Search space pruning and global optimisation of multiple gravity assist spacecraft trajectories. J. Glob. Optim. **38**, 283–296 (2006)
Jones, D.R., Perttunen, C.D., Stuckman, B.E.: Lipschitzian optimization without the Lipschitz constant. J. Optim. Theory Appl. **79**, 157–181 (1993)
Jones, D.R.: A taxonomy of global optimisation methods based on response surfaces. J. Glob. Optim. **21**, 345–383 (2001)
Kemble, S.: Interplanetary Mission Analysis and Design, Praxis Books Series. Springer, New York (2006)
Labunsky, A.V., Papkov, O.V., Sukhanov, K.G.: Multiple Gravity Assist Interplanetary Trajectories ESI Book Series. Gordon and Breach Science Publishers, London (1998)
Makino, K.: Rigorous analysis of nonlinear motion in particle accelerators. Ph.D Thesis, Michigan State University, East Lansing, Michigan, USA (1998)
Makino, K., Berz, M.: Range bounding for global optimization with Taylor models. Trans. Comput. **4**(11), 1611–1618 (2005)
Myatt, D., Becera, V., Nasuto, S., Bishop, J.: Advanced Global Optimisation for Mission Analysis and Design. Final Report, Ariadna id: 03/4101, Contract No. 18138/04/NL/MV (2004)
Peralta, F., Smith, J.C.Jr.: Cassini trajectory design description. AAS Paper 93–568, AAS/AIAA astrodynamics conference, Vistoria, B.C., Canada (1993)
Sentinella, M.R., Casalino, L.: Cooperative evolutionary algorithm for space trajectory optimization, Celestial Mech. Dynamical Astron. **105**, 211–227 (2009)
Vasile, M., Summerer, L., De Pascale, P.: Design of Earth–Mars transfer trajectories using evolutionary-branching technique. Acta Astronaut. **56**, 705–720 (2005)
Vasile, M., De Pascale, P.: Preliminary design of multiple gravity-assist trajectories. J. Spacecr. Rockets **43**, 794–805 (2006)
Yao, X.: Global optimization by evolutionary algorithms. In: Proceedings of the Second Aizu International Symposium on Parallel Algorithm Architecture Synthesis, pp. 282–291, Aizu-Wakamatsu, Japan, IEEE Computer Society Press (1997)